Available online at www.sciencedirect.com

ScienceDirect

Scripta Materialia 88 (2014) 33–36

Scripta MATERIALIA

www.elsevier.com/locate/scriptamat

Emulation of reactor irradiation damage using ion beams

G.S. Was,[a,*] Z. Jiao,[a] E. Getto,[a] K. Sun,[e] A.M. Monterrosa,[a] S.A. Maloy,[b] O. Anderoglu,[b] B.H. Sencer[c] and M. Hackett[d]

[a] *University of Michigan, 2355 Bonisteel Blvd., Ann Arbor, MI 48109, United States*
[b] *Los Alamos National Laboratory, MST-8, Ms-H816 LANL, Los Alamos, NM 87545, United States*
[c] *Idaho National Laboratory, P.O. Box 1625, MS 6188, Idaho Falls, ID 83415, United States*
[d] *TerraPower LLC, 330 120th Avenue NE Suite 100, Bellevue, WA 98005, United States*
[e] *University of Michigan, 413B Space Res Bldg., Ann Arbor, MI 48109, United States*

Received 30 March 2014; revised 21 May 2014; accepted 4 June 2014
Available online 14 June 2014

Progress in understanding radiation damage in structural materials is hampered by the lack of test reactors, long irradiations and high cost. Here we show that through strict control of experimental parameters and accounting for He production and damage-rate differences, the microstructure of ion-irradiated ferritic–martensitic steel closely resembles that created in-reactor across the full range of microstructure features. The level of agreement establishes for the first time the capability to tailor ion irradiation to emulate in-reactor radiation damage.

Keywords: Ion irradiation; Reactors; Radiation damage; Microstructure; Ferritic–martensitic alloys

Fulfillment of the promise of advanced nuclear reactors with major improvements in safety, economics, waste generation and proliferation security, and life extension of existing light water nuclear reactors rest heavily on understanding how radiation degrades the materials that serve as the structural components in reactor cores [1,2]. In high-dose fission reactor concepts such as the sodium fast reactor, core internal components must survive up to 200 dpa[1] of damage at temperatures in excess of 400 °C, Figure 1. The traveling wave reactor pushes that limit to 600 dpa. At such high damage levels, the formation and growth of voids will affect the dimensional stability of components, the nucleation and growth (or dissolution) of precipitates will alter composition locally and can either embrittle or weaken the alloy, and both phenomena are affected by the evolving dislocation microstructure [3]. In some alloys these processes develop at low doses, but void swelling and radiation-induced precipitation may emerge only after high doses (100 dpa) [4,5]. While an understanding of the microstructural evolution of alloys under irradiation remains a major challenge to the integrity of reactor core components, a more pressing problem is the diminishing capability to study these processes.

Radiation effects research is traditionally conducted by irradiating samples in test reactors, followed by comprehensive post-irradiation characterization. Predictive modeling of the radiation damage process helps to reduce the need for a full suite of experiments covering the entire parameter space. Several increasingly serious barriers are impeding the advancement of our understanding of radiation effects. The first is a paucity of worldwide test reactor capability, especially in the US, for addressing the unknowns in advanced reactor concepts. The US has only two test reactors capable of producing damage at a maximum rate of 8 dpa/year. Available reactors worldwide can only reach 20 dpa/year, making access to the required damage levels prohibitively time-consuming and expensive. Second, test reactors cannot create radiation damage significantly faster than that in commercial reactors, meaning that radiation damage research cannot "get ahead" of problems discovered during operation. Both of these factors conspire to create the third barrier: the extremely high cost of irradiation and post-irradiation characterization of highly radioactive samples.

A promising solution to the problem is the use of ion irradiation as a surrogate for neutron irradiation. Ion irradiation can yield high damage rates with negligible

* Corresponding author; e-mail: gsw@umich.edu

[1] A dpa (displacement per atom) is a unit of damage that represents the average number of times an atom is displaced from its lattice site.

http://dx.doi.org/10.1016/j.scriptamat.2014.06.003
1359-6462/

(proton irradiation) or no (heavy ion irradiation) residual radioactivity and at very low cost. The use of ion beams for radiation damage study dates back to the 1960s and includes numerous significant contributions to our understanding of radiation effects (e.g. [6–9]). The advantages of ion irradiation are many: damage rates 10^4 times that of reactor irradiation can be attained, which means that 200 dpa can be reached in days instead of decades. Because there is little or no activation samples are easily handled, reducing the cost associated with post-irradiation characterization. Control of ion irradiation experiments (temperature, damage rate, damage level) is much better than irradiations in reactor and damage can even be observed in situ. However, the idea of using ion irradiation as a surrogate for neutron irradiation is relatively new and success requires both a high degree of experiment control and a systematic approach to accounting for the differences between reactor- and accelerator-based irradiations. Capturing the full extent of the entire irradiated microstructure created in-reactor has not yet been attempted. This paper presents a "formula" for emulating reactor irradiation with well-controlled ion irradiation.

Accelerated irradiation has several challenges, the most significant being the effect of an accelerated damage rate on the resulting microstructure, and the need to account for important transmutation reactions that occur in-reactor. Gas production by transmutation can be emulated by pre-injection, or better still, by simultaneous gas implantation with damage creation. The damage rate is the larger issue and is resolved using the invariance theory derived by Mansur [10–12]. According to this theory, a change in the value of an irradiation variable from reactor conditions is accommodated by a shift in other variables with the goal of preserving the aggregate behavior of defects during irradiation. Such shifts were constructed for specific microstructure processes such as radiation-induced segregation or void growth. In both cases, the higher dose rate in an accelerator relative to a reactor requires a corresponding increase in temperature to achieve the same result [6]. The analysis assumes a steady state and that the irradiation is in either the recombination-dominant or sink-dominant regime. Damage rate differences may also result in a change in the dose to nucleation of defect clusters, but there is little theoretical or computational modeling guidance for the nucleation process. Nevertheless, a growing body of evidence for low-dose (<10 dpa) proton irradiation [13–18]has shown that the microstructural features (dislocation loops, precipitates, voids, radiation-induced segregation) and properties (hardness, stress corrosion cracking susceptibility) are in excellent agreement with reactor irradiation when the damage-rate difference is of the order of 100. We report here on the application of the theory to the high-dose and high-dose-rate regime in experiments conducted on a specific heat of ferritic–martensitic alloy HT9 that was used both in-reactor and in controlled ion irradiation experiments to determine the ion irradiation conditions that emulate the in-reactor irradiation. It is important to emphasize that both the alloy heat and heat treatments were identical for both the reactor irradiation and the ion irradiation, removing heat-to-heat variability as a potential source of disagreement (see below).

Ferritic–martensitic alloy HT9 (Fe–12Cr–1Mo) heat 84425 was used in the hexagonal fuel bundle duct labeled ACO-3, in the Fast Flux Test Facility, Hanford, WA (FFTF). It was heat treated at 1065 °C/30 min/air cooling followed by 750 °C/60 min/air cooling. The fuel bundle was irradiated in several locations in the FFTF over the time period 1985–1992 during which it accumulated a total damage of about 155 dpa at an average temperature of 443 °C [5]. Pieces from an archival section of this same duct were irradiated in a 1.7 MV tandem accelerator with self-ions (Fe^{2+}) at 5 MeV at a temperature of 460 °C and to a dose of 188 dpa determined using SRIM [19] in the Kinchin–Pease mode [20]. At this energy, Fe^{2+}ions come to rest at a depth of ~1.6 μm below the surface. The ion irradiation temperature represents a 17 °C increment above the neutron irradiation temperature, as predicted by invariance theory [12]. Temperature was closely monitored throughout the irradiation using a 2-D infrared thermal imager and ion beam current was monitored before and during the experiment. To emulate in-reactor transmutation, He was implanted prior to ion irradiation to a concentration of 1 at.ppm over a depth range of 300–1000 nm by varying the implantation energy over five different values. This amount of He was set below that generated in-reactor to compensate for the initially high He/dpa ratio in the ion irradiation experiment. Figure 2 shows the damage profile, implanted He distribution and the injected interstitial concentration as a function of depth. Note that the variation of He content is ~10% of the average and is due to the different energies used for implantation.

Principal features of the irradiated microstructure consisted of dislocation loops, precipitates and voids, which were characterized using transmission electron microscopy (TEM) with a variety of techniques: two-beam bright-field imaging (dislocation loops), dark-field imaging (precipitates), and bright-field through-focus or high-angle annular dark-field imaging (voids). Atom probe tomography (APT) was used to determine precipitate composition. Following ion irradiation, samples for characterization were made by focused ion beam (FIB) milling in cross-section to span the full depth of the irradiation. The region of the damaged zone selected for microstructure analysis (500–700 nm from the surface) was determined after considering the factors that can affect the validity of measurements. Analysis of void data in this study and MD simulations by Stoller et al. [21]have indicated that the surface effect on defects can

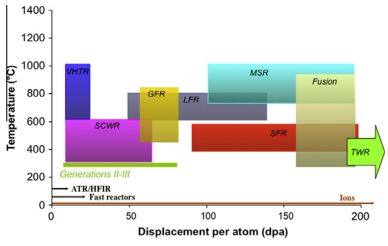

Figure 1. Schematic of the temperature-dpa requirements for various reactor concepts and the achievable annual damage rates in different test reactors and with ion irradiation. VHTR = very high temperature reactor, SCWR = supercritical water reactor, GFR = gas fast reactor, LFR = lead fast reactor, MSR = molten salt reactor, SFR = sodium fast reactor, TWR = traveling wave reactor, Generations II-III = present day light water reactors, ATR/HFIR = advanced test reactor, high flux isotope reactor.

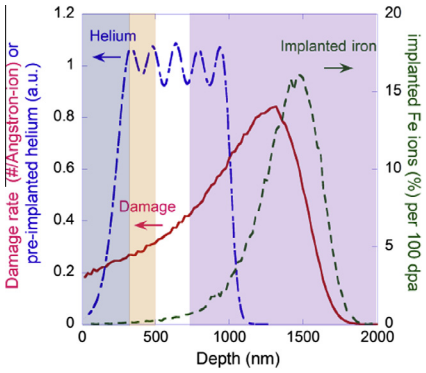

Figure 2. Selection of the region for analysis of the void microstructure (in white) in a sample of HT9 irradiated with 5 MeV Fe^{2+}. Shaded regions are excluded from analysis because of the proximity of the surface (blue), the injected interstitial (purple) and to minimize the damage variation with depth (orange). The remaining region is reduced to the unshaded area to limit the variation in damage over the region being analyzed. (For interpretation of the references to colors in this figure legend, the reader is referred to the web version of this paper.)

extend to a depth of 200–300 nm (shown as the blue shaded region in Fig. 2). The injected interstitial can suppress void swelling [22], which was found to occur beyond a depth of 700 nm (purple shaded region beyond 700 nm in Fig. 2). This leaves the region between 300 and 700 nm as free from extrinsic effects. However, to limit the variation in the magnitude of damage with depth, the 200 nm window between 500 and 700 nm (unshaded region in Fig. 2) was selected for analysis.

Figure 3a–d shows pairs of images of each feature in both ion- and reactor-irradiated samples of HT9heat 84425. Qualitatively, the microstructures show all the same radiation-produced features. In both cases, the dislocation microstructure consists of dislocation line segments (a⟨1 0 0⟩ and (a/2) ⟨1 1 1⟩) and loops, predominantly a⟨1 0 0⟩ type, of similar diameter (~20 nm) and number density ($5–9 \times 10^{20}$ m^{-3}) (Fig. 3a). Radiation-induced precipitates are primarily the G-phase as shown in the dark-field TEM image (Fig. 3b) and a Cr-rich phase (not shown). The composition of the G-phase was confirmed by APT to be close to $Mn_6Ni_{16}Si_7$. G-phase precipitates also appear along grain boundaries in both cases, as shown in the TEM bright-field images in Figure 3c. The Cr-rich phases under reactor irradiation contained only Cr, and those irradiated with Fe^{2+}consisted of Cr with a few percent carbon. Void formation is very heterogeneous in both reactor and Fe^{2+}-irradiated samples, with large variations between grains and laths. However, the size and number density were similar (Fig. 3d), as were the void size distributions (Fig. 3e).

A quantitative comparison shows the volume fraction of swelling and precipitates and the total loop line length for the ion irradiation relative to reactor irradiation (Fig. 4a), and a comparison of defect size and number density as a ratio of ion irradiation to reactor irradiation (Fig. 4b). Error bars were determined from uncertainties in size and density determination. Uncertainties in size measurements (~15%) are the standard deviation. Uncertainties in densities (~20%) are based on the uncertainties in thickness determined using the electron energy-loss spectroscopy zero-loss technique and the thickness variation across the imaged area. Errors do not include the effect of microstructure inhomogeneity. Void swelling is nearly

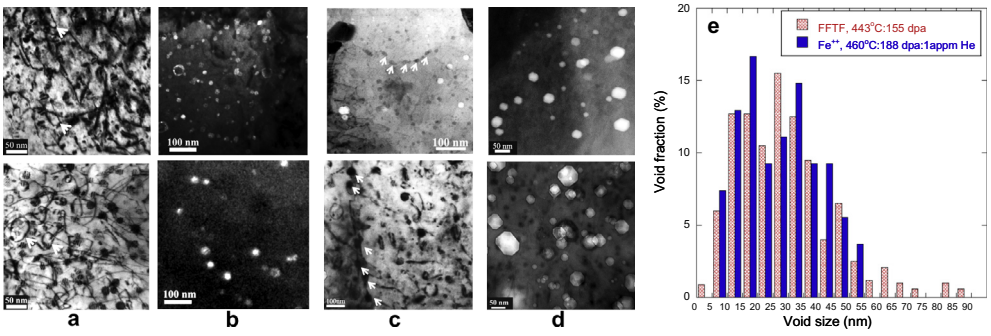

Figure 3. Comparison of irradiation microstructure in HT9 following Fe^{2+} irradiation (460 °C:155 dpa, top images) and following reactor irradiation in FFTF (443 °C:155 dpa, bottom images): (a) bright field TEM images of line dislocations and loops, (b) dark field TEM images of G-phase precipitates in the matrix, (c) bright field images of G-phase precipitates along grain boundaries, (d) voids, and (e) void size distribution for Fe^{2+} irradiation and reactor irradiation.

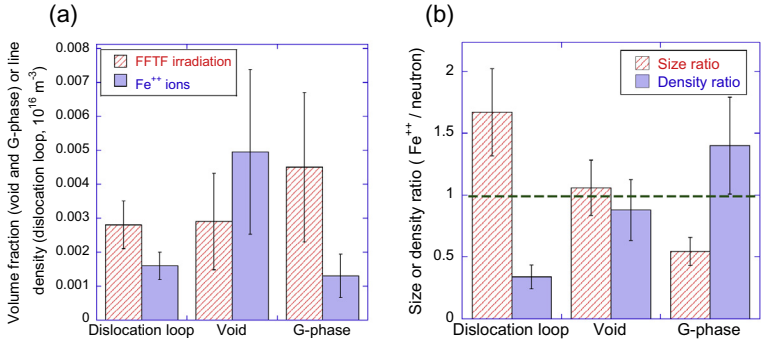

Figure 4. Comparison of (a) volume (voids, precipitates) fraction or line density (loops), and (b) size and number density ratios for ion and neutron irradiation under similar conditions.

identical between the two irradiations, and the size and density of precipitates and loops following ion irradiation are within a factor of two of those for reactor irradiation. Results indicate that, as predicted by invariance theory, the reactor-irradiated microstructure can be emulated by ion irradiation with only a modest temperature increment (17 °C). The damage increment (33 dpa) over the reactor irradiation is also small. These results indicate that an Fe^{2+} irradiation at 460 °C with pre-injection of 1 at.ppm He closely emulates the irradiated microstructure, both qualitatively and quantitatively, created by fast reactor irradiation at an average temperature of 443 °C and to a similar damage level, within the limits of measurement error and microstructure variability. When attempting to achieve agreement between experiments, the question that arises is: how close does the agreement need to be to successfully emulate the reactor irradiated microstructure?

In answering this question, it is important to consider the level of confidence in the reported damage level and temperature of the reactor irradiation. The ACO-3 duct was in-reactor for a total of seven cycles consisting of 26 segments during which it resided in four different locations in the FFTF reactor core over the period 17 August 1985–19 March 1992 [5]. As a result, it was subjected to variations in the neutron flux spectrum and temperature between cycles, resulting in a complicated damage-rate vs. temperature history and an unknown level of uncertainty in the reported dose and temperature. Available data indicate that the variation in temperature experienced by this duct over its lifetime may be 40–50 °C.

It is well known that irradiated microstructures can be quite sensitive to damage-rate vs. temperature history and that reactor startups and shutdowns can introduce complexity into the irradiated microstructure not seen when both are fixed for the entire irradiation. Kiratani et al. [23] showed that the dislocation and void microstructures of Ni-base alloys could vary by factors of up to 2× in size and 20× in number density just by varying the temperature during reactor startup and shutdown. Their example shows how subtle differences in reactor operation can lead to large differences in the irradiated microstructure. Thus, the complicated dose–temperature history of the ACO-3 duct introduces considerable uncertainty into the average irradiation temperature. Reactor irradiations can and should be conducted with precise temperature control. Only then can they be used to better inform constitutive models of material performance as well as validate ion irradiation as a tool for emulation of reactor irradiation. Experiments are under way to generate reactor data with a high degree of control and stability at the sample locations on a range of model and commercial alloy samples [24]. In fact, commercial reactor components will always undergo complicated damage-rate vs. temperature histories during their operation. Thus, the burden of comparison between ion and reactor irradiations must fall on the development of ion irradiation to take account of the operational variability in-reactor, otherwise, its utility as a predictive tool will not be fulfilled.

High-dose ion irradiation of a ferritic–martensitic steel shows that well-controlled experiments that account for the differences between reactor- and accelerator-based irradiations can create the same radiation-produced defect clusters with similar sizes and number densities as those created in-reactor. While a comprehensive theoretical framework is still lacking, these results provide optimism that ion irradiations can be tailored to emulate the full suite of radiation defects in a reactor environment, thus greatly speeding the development of materials to enable development of advanced reactor concepts.

The authors thank OvidiuToader of the Michigan Ion Beam Laboratory for assistance with ion irradiations and MychailoToloczko of PNNL for temperature history calculations of the duct. This work was supported by the US Department of Energy through award DE-AC07-05ID14517, TerraPower Inc. through research roundtable agreement DRDA 11-PAF05786, and the NSF Graduate Research Fellowship Program through award #DGE 1256260, and NSF grant #DMR-9871177 for support of the JEOL2010F TEM.

[1] G.S. Was, Fundamentals of Radiation Materials Science: Metals and Alloys, SpringerVerlag, Berlin, 2007.
[2] Z. Jiao, G.S. Was, J. Nucl. Mater. 425 (2012) 105–111.
[3] B.H. Sencer, J.R. Kennedy, J.I. Cole, S.A. Maloy, F.A. Garner, J. Nucl. Mater. 393 (2009) 235–241.
[4] M. Kiritani, T. Yoshiie, S. Kojima, Y. Satoh, K. Hamada, J. Nucl. Mater. 174 (1990) 327–351.
[5] Applied Physics Society Panel of Public Affairs, Extending Licenses for the Nation's Nuclear Power Plants, 2013.
[6] US DOE Nuclear Energy Research Advisory Committee and the Generation IV International Forum, A Technology Roadmap for Generation IV Nuclear Energy Systems, 2002.
[7] S.J. Zinkle, S. Kojima, J. Nucl. Mater. 179–181 (1991) 395–398.
[8] P.R. Okamoto, L.E. Rehn, J. Nucl. Mater. 83 (1979) 2–23.
[9] R.S. Averback, J. Nucl. Mater. 108–109 (1982) 33–45.
[10] Proc. Workshop of Neutron and Charged Particle Damage, CONF-760673, Oak Ridge National Laboratory, Oak Ridge, TN, 8–10June 1976, p. 147.
[11] L.K. Mansur, Nucl. Technol. 40 (1978) 5–34.
[12] L.K. Mansur, J. Nucl. Mater. 78 (1978) 156–160.
[13] L.K. Mansur, J. Nucl. Mater. 206 (1993) 306–323.
[14] G.S. Was, J. T. Busby, T. Allen, E. A. Kenik, A. Jenssen, S. M. Bruemmer, J. Gan, A. D. Edwards, P. Scott and P. L. Andresen, J. Nucl. Mater. 300 (2002) 198–216.
[15] G.S. Was, M. Hash, G.R. Odette, Phil. Mag. 85 (4–7) (2005) 703–722.
[16] L. Fournier, A., Serres, Q., Auzoux, D., Leboulch, G.S., Was, J. Nucl. Mater. 384 (2009) 98.
[17] L. Tournadre, F. Onimus, J.-L. Béchade, D. Gilbon, J.-M. Cloué, J.-P. Mardon, X. Feaugas, O. Toader, C. Bachelet, J. Nucl. Mater. 425 (2012) 76.
[18] X.T. Zu, K. Sun, M. Atzmon, L.M. Wang, L.P. You, F.R. Wan, J.T. Busby, G.S. Was, R.B. Adamson, Phil. Mag. 85 (2005) 649.
[19] R. Schaublin, M., Victoria, J. Nucl. Mater. 283–287 (2000) 339.
[20] R.E. Stoller, J. Nucl. Mater. 307–311 (2002) 935–940.
[21] F.A. Garner, J. Nucl. Mater. 117 (1983) 177–197.
[22] US Department of Energy, <https://inlportal.inl.gov/portal/server.pt/community/neup_home/600/fy13_irp_awards> 2013.
[23] J.F. Ziegler, M.D. Ziegler, J.P. Biersak, Nucl. Instr. Meth. Phys. Res. B268 (2010) 1818–1823.
[24] R.E. Stoller, M.B. Toloczko, G.S. Was, A.G. Certain, S. Dwaraknath, F. Garner, Nucl. Instr. Meth. Phys. Res. B 310 (2013) 75–80.